Corresponding IVUS and Angiogram Image Data

D Rotger, P Radeva, C Cañero, JJ Villanueva,
J Mauri†, E Fernández†, A Tovar†, V Valle†
Computer Vision Center, University Autonoma of Barcelona, Bellaterra, Spain
† University Hospital Germans Trias i Pujol, Badalona, Spain

Abstract

The growing appreciation of the pathophysiological and prognostic importance of arterial morphology have led to the realization that angiograms are inherently limited in defining the distribution and extension of coronary wall disease. By IntraVascular UltraSound (IVUS) physicians have a picture of the composition of vessel in detail. However, observing an IVUS pullback it is difficult to figure out the catheter position with regard to the vessel parts and ramifications, and misclassification of lesions is possible. The objective of this work is to develop a computer vision technique to fuse the information from IVUS and angiograms defining the correspondence of every IVUS image with a corresponding point of the vessel in the angiograms.

1. Introduction

Intravascular ultrasound images have allowed deepening in the knowledge of the true extension of the coronary vessel illness. The tomographic image that provides a unique 2D *in vivo* vision of the internal vessel walls (figure 1.a), determining the extension, distribution and treatment of the atherosclerotic, fibrotic plaques and thrombus, and their possible repercussion on the internal arterial lumen. Angiography images provide an external vision of the vessel shape and tortuosity (figure 1.b). The main advantage of the ultrasound compared to the angiography images, deals with the fact that the most of the visible plaque lesions with IVUS are not evident with angiogram.

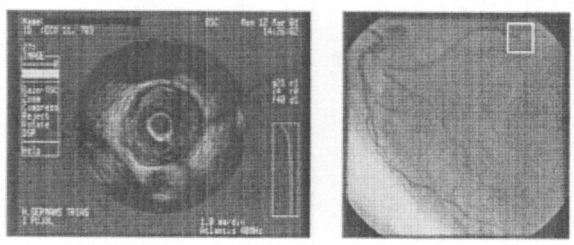

(a) (b)

Figure 1. (a) IVUS image. (b) Angiography of a vessel with stenosis.

Studies on intravascular ecography have shown that the reference vessel segment has the 35-40% of its sectional area occluded because of the plaque, although it appears as normal in the angiography. Besides its capacity of demonstrating the plaque extension and distribution inside the vessels, IVUS offer information about the composition of the internal lesion; in particular, about calcium deposits as the most important isolated predictors to evaluate if a particular lesion will respond to a catheter treatment.

The studies about stents[1] carried out with IVUS show that the appearance in the angiography of a good stent deployment can hide two possible problems: the incomplete apposition (a portion of the stent is not making pressure on the vessel wall) and the incomplete expansion (a portion of the stent remains closed although the expansion of the rest of the stent areas). Both problems are very significant since they can be worse than the problem they are trying to solve.

Both methods (IVUS and angiogram) provide a lot of information about the internal and the external shape of the coronary vessels respectively. The fusion of all this information will allow the physicians to interact with the real extension and distribution of the disease in the space, making easier the arduous task of having to imagine it.

One of the problems of dealing with IVUS is the fact that the images represent an 2D plane perpendicular to the catheter without any depth information. This IVUS property hides the real disease's extension and represents a very unnatural way of conceptualization. The foremost limitation of IVUS on the pre- and post-treatment studies is the lesion images correlation in the serial studies. This limitation is due to the lack of the third dimension that gives much more global information about the internal and external vessel structure. This problem can be solved by using the information given by the angiographies. Using two angiogram projections and taking into account the calibration parameters, we are able to create a curve in the space, representing the vessel tortuosity, where placing the IVUS images and a deformable model representing the vessel wall, the intimal layer or the stent between these planar images.

[1] Spiral metallic mesh implanted inside a coronary vessel to save the stenosis effect

0276-6547/01 $17.00 © 2001 IEEE

Computers in Cardiology 2001;28:273-276.

2. Biplane system

The first thing we need to do is defining a biplane system with the angiograms. We could have a biplane angiocardiographic equipment consisting of two X-ray imaging systems, i.e., a frontal and a lateral system (figure 2). The projection axes of both systems intersect in the *isocenter*. The distances from the X-Ray sources to the image intensifiers are predetermined before the image acquisition process. To create our biplane system, we have followed the steps explained in the articles [1, 2, 3].

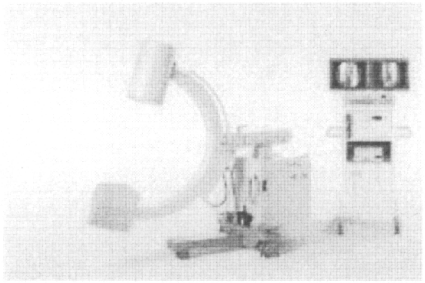

Figure 2. Siemens C-Arm angiocardiographic system.

So we are able to create a model of the vessel tortuosity in the space by pointing some of its points on one image and their corresponding ones on the other image by using the epipolar line as a guide (figure 3) and using them to generate a three-dimensional B-Spline curve. To do that we extrapolate the control points of the B-Spline from the given points. [4]

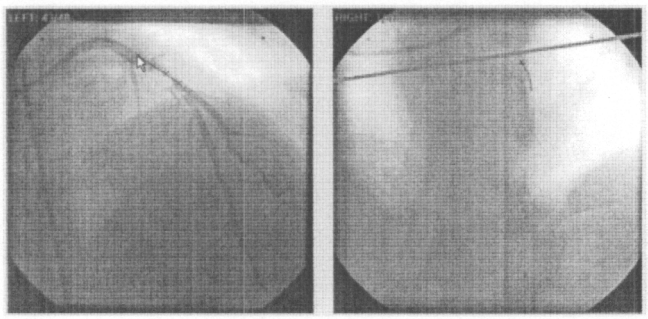

Figure 3. Pointing one position on a projection plane and its corresponding epipolar line on the other.

3. IVUS models

Models of the vessel wall, the intimal layer and the stent are very useful in order to determine vessel morphology in the space, to extract volumetric measurements and to take decision about stent implantation. These models have been implemented by B-Splines because of their nice properties (easy to adapt to the vessel's morphology, local control, model compactness, etc.). Using aperiodic and periodic blending functions, we obtain a cylindrical topology of our model.[4]

The models can be easily generated by determining the position of the B-Spline control points which define a curve to adjust manually or automatically [5] to vessel wall, intimal layer and stent boundaries in each of the IVUS images. If we assume the section we are treating as straight we can generalize two-dimensional models on the image planes to three-dimensional ones. We can create a NURBS[2] surface by using the control points of each image to be its knots (figure 4). [6]

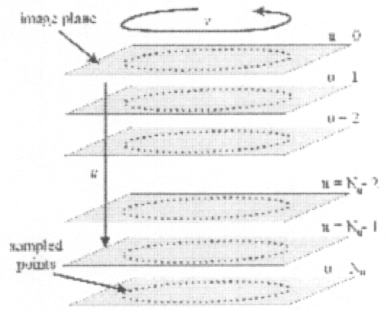

Figure 4. Two-dimensional B-Spline model space generalization.

Distance between each image (plane) is determined by IVUS catheter pullback speed and the digitalization parameter of discretization (the images are saved in an SVHS videotape and digitized, normally at 25 frames per second). Then we just have to place each IVUS plane at the given distance and situate its control points on it.

4. Models fusion

4.1. Pullback curve and vessel shape

The first thing we have to do is creating a curve model of the pullback on the angiographies. For this purpose we need two projections with the catheter stopped before the pullback begins (BPB) and another two at the end. We can create a curve model of the pullback situating one model extreme at the position of the ultrasound transducer at PBP and, changing to PAP, situate the ending extreme of the model coinciding with the last position of the catheter during its pullback.

Given that the heart is moving it is difficult to find four projections (two before and two after the pullback) with the coronary vessels in the same situation. To ease this issue, we use the electro-cardiogram (ECG), given from the DICOM angiography images, which allows us choosing the

[2]Non Uniform Rational B-Spline

images of each projection sequence corresponding to the same situation of the cardiac cycle (figure 5).

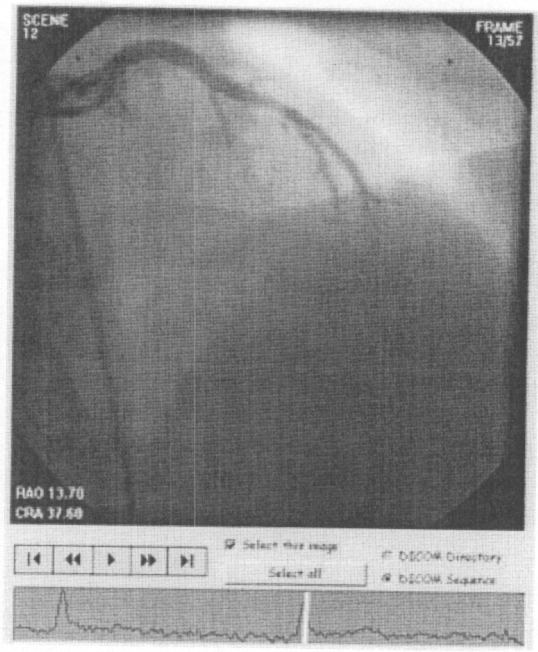

Figure 5. Image of the projection sequence and its ECG.

Once we have four projections of the catheter in the same situation of the cardiac cycle, we can create the B-Spline model of the pullback as described in section 2. Next step is creating and adjusting the models of the vessel wall, the intimal layer and the stent along the IVUS images sequence as described on section 3.

4.2. Registration

Having a model of the curve the vessel describes in the space, coming from the angiographies, and another one of its internal composition, coming from the IVUS images, we are in a position to fuse both models into one showing the internal shape of the vessel and its tortuosity in the space.

Due to our work with an IVUS phantom proportioned by Boston Scientific Corporation, we have seen it is easy to identify different speed cycles of the catheter during its pullback. This will determine the way of placing the IVUS images along the pullback curve as we will see later. There is a significant delay from the moment the pullback machine is switched on and the moment the catheter really starts its pullback (cycle 1). It is caused because the catheter is quite thin and when pushed into the vessel it describes little waves. When the pullback starts, it stretches first and then it starts its movement. Then, there is an acceleration cycle (cycle 2) preceding the constant movement of the catheter. The last cycle detected comes from the delay of the instant when the pullback machine is switched off and when the catheter really stops (cycle 4). The appreciation of this cycles and their duration has been estimated from 13 angiogram pullback image sequences, by indicating the switching on and the switching off of the pullback machine in the images with a marker. The results of this study have been: an average time 5.077 seconds for the switch on cycle, an average time 0.6154 seconds for the acceleration one and an average of 0 seconds for the cycle 4 as figure 6 shows. This has led us to place the IVUS images from the end of the pullback curve.

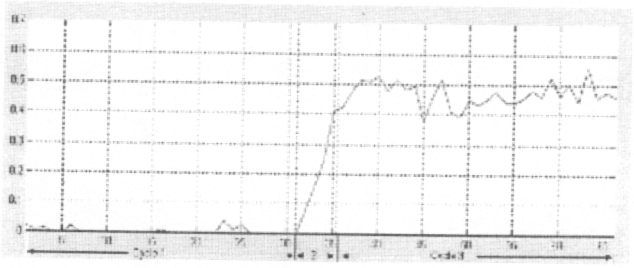

Figure 6. Pullback cycles estimation.

Taking into account these cycles, we can start situating the IVUS images along the 3D curve we have created. As we have said, the position corresponding to the center of the catheter of the last IVUS image of the pullback will be placed at the curve extreme corresponding to the ending of the pullback. We can go on situating the other images along the curve at a distance given by the pullback speed and the images discretization. The X and Y axis of the images will correspond, respectively, to the normals and binormals of the 3D curve at that point. Given that we are using B-Splines, we will use Blending function's formulas[4]:

$$Q(u) = \frac{1}{6} \begin{pmatrix} 1 \\ u \\ u^2 \\ u^3 \end{pmatrix} \begin{bmatrix} 0 & 1 & 4 & 1 \\ 0 & 3 & 0 & -3 \\ 0 & 3 & -6 & 3 \\ 1 & -3 & 3 & -1 \end{bmatrix} \begin{pmatrix} v_0 \\ v_1 \\ v_2 \\ v_3 \end{pmatrix} \quad (1)$$

where $\vec{v}$ are the span vertices.

The tangent ($\vec{t}$) and the normal ($\vec{n}$) vectors at Q(u) are defined as:

$$\vec{t} = Q'(u) \qquad \vec{n} = Q''(u)$$

To make $\vec{t}$ and $\vec{n}$ orthonormals:

$$\vec{n} = (\vec{t} \times \vec{n}) \times \vec{t}$$

And so the binormal vector is defined as:

$$\vec{b} = \vec{t} \times \vec{n}$$

So using (1) we are able to calculate the position of any point of the curve in the space by using the appropriate $\vec{v}$ and incrementing the internal variable u. If the increments

of u are small enough we can calculate the length of a segment of the curve by accumulating the calculus of the Euclidean distance between all the consecutive points of the segment. When this distance is equal or greater than the distance between two IVUS images, we will place there the center of the next IVUS plane orienting its vertical axis by $\vec{n}$ and the horizontal one by $\vec{b}$.

In order to soften the rotational effect between two consecutive planes, we can project the normal and binormal vectors of the previous plane to the actual one:

$$\vec{t_i} = \vec{n_i} \times \vec{b_i}$$

$$\vec{n_i} = \vec{n}_{i-1} - \vec{t_i} * (\vec{n}_{i-1} \cdot \vec{t}_{i-1})$$

$$\vec{b_i} = \vec{t_i} \times \vec{n_i}$$

Once we have the IVUS planes oriented in the space we can show the IVUS models oriented as the planes by placing the 3D control points on each position on the planes (figure 7).

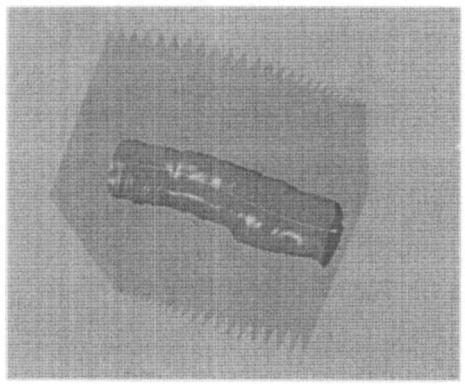

Figure 7. Vessel model placed in the space.

Now we have placed all the IVUS images along the 3D curve the catheter describes along its pullback. The next thing we can do, when knowing where the IVUS images are, is showing the IVUS image corresponding to given point of the angiography. The user has to select a point on the angiography and its correspondent on the other projection by using the epipolar line. Then, doing a back-propagation of the given points, we will have the point in the space. The next thing we have to do is verifying that the point is on the pullback model and, if not, finding the point of the 3D model nearest to the selected one. Once we have the position of the desired point on the 3D model of the pullback, the last thing to do is finding the nearest IVUS image to the point. As we have the 3D position of the center of each IVUS image the only thing we have to do is to calculate the shorter segment of the curve to find an image. We do not use euclidean distance because the curve is not assumed to be straight between two images.

5. Results and conclusions

In order to validate the proposed approach disregarding the artifacts coming from the vessel motion, we used 13 IVUS pullbacks on a phantom provided by Boston Scientific with a calcium deposit (CD). Once detected the CD on the IVUS image, we estimated its position in space and tested its appearance from the angiograms. The error of CD estimate was 0.3mm explained by the manual annotation of pullback "start" and "end" as well as the impossibility of recording it with precision higher than a second in the current IVUS acquisition systems.

We have also tested the system with 3 real cases of patients in the University Hospital "Germans Trias i Pujol" (Badalona, Spain) with an estimated error of 1.027mm according to the pullback length compared to the reconstructed curve length.

To sum up, fusing IVUS and angiogram data is of high clinical interest to help the physician locate lesions in IVUS data and decide how long it is, how far from a bifurcation or another lesions it lays, etc. In this study, we developed tools to estimate and show the correspondence between IVUS images and vessels in angiograms and have validated it on an IVUS phantom and with real cases with very encouraging results.

References

[1] et al. AD. Determination of optimal angiographic viewing angles: Basis principles and evaluation study. IEEE Medical Imaging 1994;13:13–23.

[2] et al. PR. 3d vessel reconstruction from biplane angiograms using snakes. In Computers in Cardiology 1998, volume 25. IEEE Computer Society Press, 1998; 773–776.

[3] et al. CC. 3d curve reconstruction by biplane snakes. In 15 th International Conference on Pattern Recognition, Barcelona, volume 4. 2000; 563–566.

[4] et al. B. An Introduction to Splines for use in Computer Graphics and Geometry Modeling. Morgan Kaufmann Publishers INC, 1987.

[5] et al. DG. Authomatic segmentation of artery wall in coronary ivus images: A probabilistic approach. In Computers in Cardiology 2000, volume 27. IEEE Computer Society Press, 2000; 687–690.

[6] et al. PR. 3d reconstruction of a stent by deformable models. In Visualisation, Imaging, and Image Processing, IASTED. 2001; 417–422.

Address for correspondence:

David Rotger Muñoz
Computer Vision Center / Edifici O / Campus UAB
08193, Bellaterra (Spain)
rotger@cvc.uab.es